



Synthesis of nanosized $\text{TiO}_2/\text{SiO}_2$ particles in the microemulsion and their photocatalytic activity on the decomposition of *p*-nitrophenol

Seong-Soo Hong*, Man Sig Lee, Seong Soo Park, Gun-Dae Lee

Division of Chemical Engineering, Pukyong National University, 100 Yongdang-dong, Nam-ku, Pusan 608-739, South Korea

Abstract

Nanosized pure TiO_2 particles were prepared by hydrolysis of TTIP in the sodium bis(2-ethylhexyl)sulfosuccinate (AOT) reverse micelles. $\text{TiO}_2/\text{SiO}_2$ nanoparticles were also prepared from TEOS as a silicon source and TTIP as a titanium source. These particles were characterized by TEM, XRD, FT-IR, BET, TGA and DTA. From thermal analysis and XRD analysis, the anatase structure of pure titania appeared in the 300–600 °C calcination temperature range and the rutile structure was showed above 700 °C. However, no rutile phase was observed for the $\text{TiO}_2/\text{SiO}_2$ particles up to 800 °C. The crystallite size decreased and the surface area of $\text{TiO}_2/\text{SiO}_2$ particles monotonically increased with an increase of the silica content. From FT-IR analysis, the band for Ti–O–Si vibration was observed and the band intensity for Si–O–Si vibration increased with an increase of the silica content. The micrographs of TEM showed that the $\text{TiO}_2/\text{SiO}_2$ nanoparticles had a spherical and a narrow size distribution. In addition, $\text{TiO}_2/\text{SiO}_2$ particles showed higher photocatalytic activity than pure TiO_2 and the $\text{TiO}_2/\text{SiO}_2$ (90/10) particles showed the highest activity on the photocatalytic decomposition of *p*-nitrophenol.

© 2003 Elsevier B.V. All rights reserved.

Keywords: Nanosized $\text{TiO}_2/\text{SiO}_2$ particles; AOT; Reverse micelle; W_0 ratio

1. Introduction

Particles smaller than tens of nanometers in primary particle diameter (nanoparticles) are of interest for the synthesis of new materials because of their low melting point, special optical properties, high catalytic activity, and unusual mechanical properties compared with their bulk material counterpart [1].

Many methods have been developed to control the size of nanoparticles such as Langmuir–Blodgett films [2], vesicles [3], reverse microemulsions [4] and

surface-active supports [5]. Microemulsions provide a microheterogeneous medium for the generation of nanoparticles. The formation of particles in such systems is controlled by the reactant distribution in the droplets and by the dynamics of interdroplet exchange. The surfactant stabilized microcavities provide a cage-like effect that limits particle nucleation, growth and agglomeration [6,7]. In addition, water-in-oil (w/o) microemulsions have been successfully employed to obtain ultrafine particles of controlled size of a variety of materials [8,9].

Anderson and Bard [10] reported the effect of incorporation of silica on the behavior of the titania-based photocatalyst prepared by a sol–gel technique. According to the result for the decomposition of

* Corresponding author. Tel.: +82-51-620-1465;

fax: +82-51-625-4055.

E-mail address: sshong@pknu.ac.kr (S.-S. Hong).

rhodamine-6G, the titania/silica mixed oxide with the ratio of 30/70 produces the highest activity about three times higher than Degussa P25 titania.

In the present work, the nanosized pure TiO_2 and the nanosized $\text{TiO}_2/\text{SiO}_2$ particles were prepared using TTIP and TEOS as precursors in the sodium bis(2-ethylhexyl)sulfosuccinate (AOT) reverse microemulsion. In addition, their photocatalytic activity on the decomposition of *p*-nitrophenol was also examined.

2. Experimental

The preparation method of the pure titania particle was followed by the previous report [9]. Titania/silica particles were prepared by the water-in-oil microemulsion. Titanium tetraisopropoxide (TTIP, 98% Aldrich) and tetraethylorthosilicate (TEOS, 98% Aldrich) were used as precursors of titania and silica, respectively. Cyclohexane (Oriental Chemical Industries) was used as an organic solvent. Water used in the experiments was doubly distilled and deionized. The water/surfactant (W_0) molar ratio and water/TTIP + TEOS (R) molar ratio were maintained at 1 and 2, respectively.

Nanosized $\text{TiO}_2/\text{SiO}_2$ particles were prepared by the controlled hydrolysis of TTIP and TEOS in water-in-oil (w/o) microemulsions stabilized with the anionic surfactant AOT. Reverse microemulsion solution was prepared by dissolving 0.045 mol of surfactant in cyclohexane and by adding a required amount of distilled water. The water-clear appearance of the solution indicated the formation of the microemulsion. The hydrolysis rate of TEOS is much slower than that of TTIP. Therefore, TEOS was hydrolyzed in the first step with the pre-mixed reverse microemulsion solution. After the two precursors were added in the pre-mixed solution, it was mixed for 4 h to obtain $\text{TiO}_2/\text{SiO}_2$ particles. The hydrolysis reaction was carried out at 30 °C in a sealed four-way flask (500 ml). The $\text{TiO}_2/\text{SiO}_2$ particles precipitated were separated in a centrifuge at 10,000 rpm for 2 min and were then washed with ethanol using Soxhlet extractor for 24 h to remove organic compounds and surfactants from the particles. The particles were dried in the oven at 105 °C for 12 h and calcined between 300 and 800 °C for 3 h.

A biannular quartz glass reactor with a UV lamp immersed in the inner part was used for all the photocatalytic experiments. The batch reactor was filled with 500 ml of an aqueous dispersion in which the concentration of $\text{TiO}_2/\text{SiO}_2$ particles and of *p*-nitrophenol were 0.1–0.4 g/l and 10–100 mg/l, respectively and magnetically stirred to maintain uniform concentration and temperature. A 1000 W high pressure mercury lamp (Kumkang Co.) was used. The circulation of water in the quartz glass tube between reactor and lamp allowed to cool the lamp and to warm the reactor at the desired temperature. Nitrogen was used as a carrier gas and pure oxygen was used as an oxidant. The samples were immediately centrifuged and the quantitative determination of *p*-nitrophenol was performed by UV-Vis spectrophotometer (Shimadzu UV-240).

The dried fine powders of synthesized TiO_2 were subjected to thermo gravimetric-differential thermal analysis (TG-DTA, Perkin-Elmer) to determine the temperature of possible decomposition and phase change. The chemical structure of the prepared particles was examined using Fourier transform infrared spectrophotometer (FTIR, Bruker, IFS-88). The major phase of the obtained particles was analyzed by X-ray diffraction (Rigaku D/MAXIC) using $\text{Cu K}\alpha$ radiation. Crystallite size of the prepared particles was determined from the broadening of the anatase main peak at $2\theta = 25.3^\circ$ by the Scherrer equation [11]. Surface area of the prepared particles was determined by nitrogen physisorption data at 77 K using a Micromeritics ASAP 2400 and pore volume was determined by the BJH (Barrett-Joyner-Halenda) method. The particle size and external morphology of the prepared particles were observed by transmission electron microscopy (TEM, JEOL, JEM-2020).

3. Results and discussion

3.1. Thermal analysis

Fig. 1 shows the DTA and TGA thermodiagrams for the pure TiO_2 and $\text{TiO}_2/\text{SiO}_2$ nanoparticles. From the TGA analysis of the pure TiO_2 , the weight of particles sharply decreases up to 350 °C and slowly decreases from 350 to 900 °C.

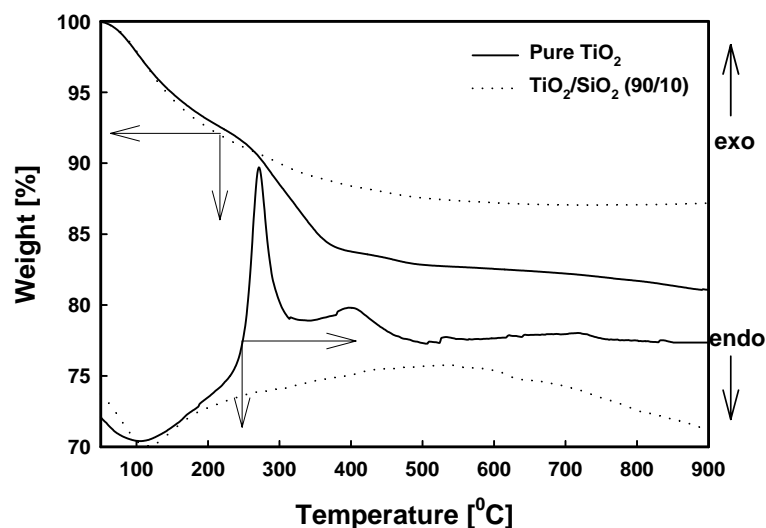


Fig. 1. DTA–TGA curves of the pure TiO_2 and $\text{TiO}_2/\text{SiO}_2$ nanoparticles prepared at different TTIP/TEOS ratio.

DTA analysis of the pure TiO_2 also shows the endothermic peak at 100°C and two exothermic peaks at 280 and 390°C . It is thought that the peak at 100°C is due to free adsorbed water, and the peak at 280°C is due to the decomposition of the surfactant and residual hydroxy group. In addition, the peak at 390°C corresponds to the crystallization of the amorphous phase into the anatase phase. Above 450°C , it can be assumed that the product completely transforms into the anatase phase because there is no change in particle weight. In the titania particles prepared using AOT reverse microemulsion, it is confirmed that the anatase phase begins to transform into the rutile phase at 700°C from the XRD results.

The $\text{TiO}_2/\text{SiO}_2$ particles indicates a prominent endothermic peak below 100°C due to free adsorbed water and a exothermic peak at 500°C corresponds to the crystallization of the amorphous phase into the anatase phase. It is also confirmed that no rutile phase appears up to 800°C from the XRD results. Thereafter no significant thermal effects can be detected even up to 1000°C .

3.2. X-ray diffraction analysis

Fig. 2 shows the XRD patterns of nanosized TiO_2 and $\text{TiO}_2/\text{SiO}_2$ (90/10) particles calcined at different temperature. The major phase of all the pure TiO_2

particle is an anatase structure and a rutile peak was observed above 700°C . For $\text{TiO}_2/\text{SiO}_2$ particle, however, no significant rutile phase was observed although the calcination temperature was over 800°C . In addition, no peak for the silica crystal phase was observed at all calcination temperature.

The crystallite size of particles prepared by different calcination temperature is summarized in Table 1. One can see that the crystallite size of the anatase phase of the pure titania increased from 8 to 47 nm, but that of $\text{TiO}_2/\text{SiO}_2$ particles slowly increased from 6 to 14 nm as the calcination temperature increased

Table 1
Physical properties of nanosized powders calcined at various temperatures

Calcination temperature ($^\circ\text{C}$)	XRD			
	Pure TiO_2^a		$\text{TiO}_2/\text{SiO}_2$ (90/10) ^b	
	Structure	Crystallite size ^c (nm)	Structure	Crystallite size ^c (nm)
400	Anatase	8	Anatase	6
500	Anatase	11	Anatase	7
600	Anatase	14	Anatase	8
700	Anatase/rutile	25	Anatase	10
800	Rutile/anatase	47	Anatase	14

^a $W_0 = 0.5$; $R = 2$.

^b $\text{TiO}_2/\text{SiO}_2$ ratio = 90/10; $W_0 = 1$; $R = 2$.

^c Obtained by Scherrer equation.

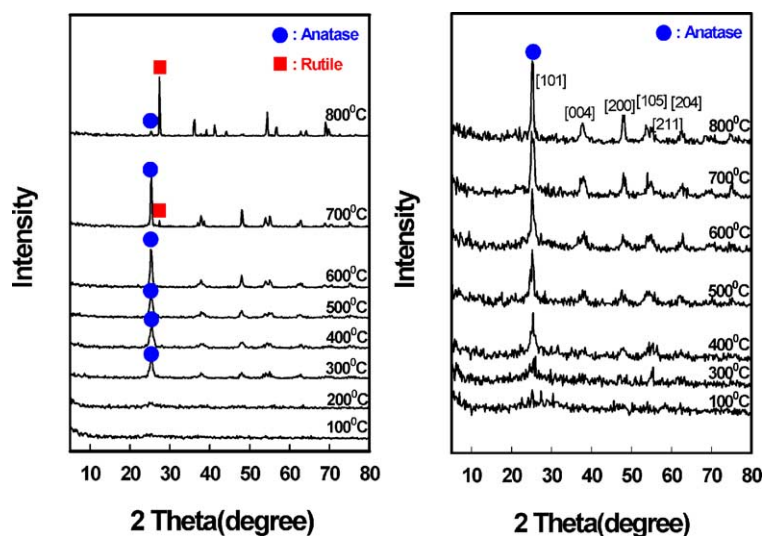


Fig. 2. XRD patterns of the pure TiO_2 (a) and $\text{TiO}_2/\text{SiO}_2$ (90/10) (b) nanoparticles calcined at different temperatures.

from 400 to 800 °C. This result indicates that the addition of SiO_2 in titania particle decreased the crystallite size and crystallinity by inhibiting the growth of the titania particles. It is well known that the calcination improves the crystallinity of the particle, and the amorphous TiO_2 changes into the anatase phase and the anatase phase changes into the rutile phase with an increase of calcination temperature [8]. In addition, the particle size decreases and the crystallinity of the particle enhances with an increase of calcination temperature. It is also confirmed that the titania/silica mixture has high thermal stability, which results in the suppression of phase transformation of titania from anatase to rutile. In addition, this high thermal stability made it possible to calcine the $\text{TiO}_2/\text{SiO}_2$ particles at higher temperature without forming the rutile phase and to prepare high crystalline particles with reducing the bulk defects.

3.3. FT-IR analysis

Fig. 3 shows the FT-IR spectra for nanoparticles prepared by different TTIP/TEOS molar ratio at W_0 ratio 1, R ratio 2 and calcined at 500 °C.

The wave number of 940–960 and 1080–1105 cm^{-1} in Fig. 3 indicate the band for Ti–O–Si and Si–O–Si bond, respectively [12]. When the SiO_2 content is over 10%, the band for Ti–O–Si vibration is observed. The

band intensity for Si–O–Si vibration increases with an increase of the silica content. This result suggests that the silica exists as a segregated amorphous phase in the anatase titania particles and some fraction of metal–O–metal bonding are Ti–O–Si.

The broad absorption peak appearing near 3400 cm^{-1} relates to a stretching vibration of Ti–OH group. At 1620 cm^{-1} , a band assigned to water also appears. The intensities of absorption peaks due to O–H group near 1620 and 3400 cm^{-1} increased with an increase of the silica amount and it shows similar tendency with the result of Jung and Park [13].

3.4. TEM analysis and surface area

Fig. 4 shows the TEM micrographs of the nanoparticles prepared by different TTIP/TEOS molar ratio at W_0 ratio = 1, R ratio = 2 and calcined at 500 °C. The micrographs show that the nanoparticles have a spherical and a narrow size distribution. The crystallite size of particles decreases with an increase of the SiO_2 content and is listed in Table 2. The crystallite size was determined by counting the number of particle size in a given area and that was 10 nm at pure TiO_2 and decreased to 4 nm at $\text{TiO}_2/\text{SiO}_2$ (70/30) particles. The crystallite sizes calculated from XRD analysis are nearly the same as those obtained from TEM analysis. This result suggests that the crystallite size of

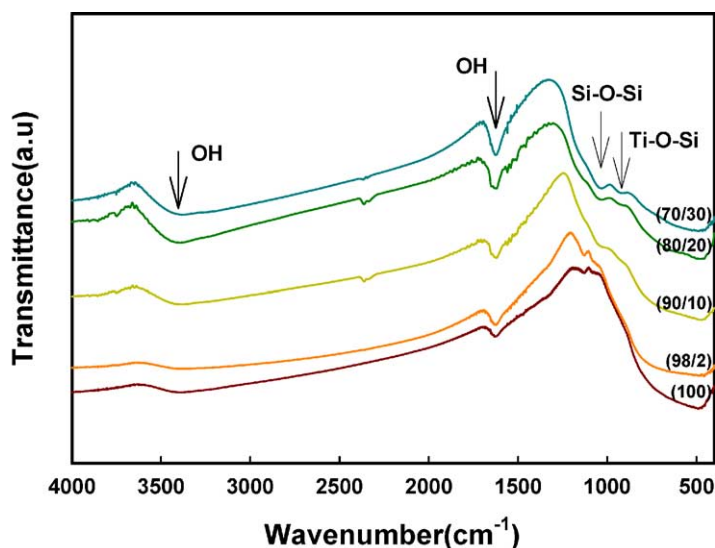


Fig. 3. FT-IR spectra of the pure TiO_2 and $\text{TiO}_2/\text{SiO}_2$ nanoparticles prepared at different TTIP/TEOS ratio.

$\text{TiO}_2/\text{SiO}_2$ particles prepared by the w/o microemulsion is found to depend on the silica content and the addition of silica in $\text{TiO}_2/\text{SiO}_2$ particle inhibits the growth of the titania crystals.

BET surface area of the $\text{TiO}_2/\text{SiO}_2$ particles calcined at 500°C are shown in Table 2 as a function of the silica content. It can be seen in Table 2 that the surface area rapidly increases with an increase of the silica content from 72 for pure TiO_2 to $275\text{ m}^2/\text{g}$ for the $\text{TiO}_2/\text{SiO}_2$ (70/30) particles. This result indicates that the addition of amorphous silica into titania matrix helps to suppress the reduction of surfaces area at high calcination temperature.

3.5. Activity test

It is well known that photocatalytic oxidation of organic pollutants follows Langmuir–Hinshelwood kinetics [14]. Therefore, this kind of reaction can be represented as follows:

$$-\frac{dc}{dt} = kC \quad (1)$$

In addition, it can be integrated as follows:

$$C = C_0 \exp(-kt) \quad (2)$$

where C_0 is the initial concentration of the *p*-nitrophenol and k is a rate constant related to the reaction

Table 2

Physical properties of nanosized $\text{TiO}_2/\text{SiO}_2$ particles prepared at different TTIP/TEOS ratio and their photocatalytic activity for the degradation of *p*-nitrophenol

Catalyst ^a ($\text{TiO}_2/\text{SiO}_2$ ratio)	XRD, crystallite size ^b (nm)	TEM, crystallite size (nm)	BET		Activity ^c , $k \times 10^{-3}$ (min^{-1})
			Surface area (m^2/g)	Pore volume (cm^3/g)	
100	10	10	72	0.13	1.3
98/2	8	8	110	0.16	1.4
90/10	7	7	189	0.26	1.8
80/20	6	6	239	0.22	1.2
70/30	4	<4	275	0.21	0.9

^a $W_0 = 1$; $R = 2$; calcination temperature = 500°C .

^b Obtained by Scherrer equation.

^c Apparent first-order constant (k) of photocatalytic degradation of *p*-nitrophenol.

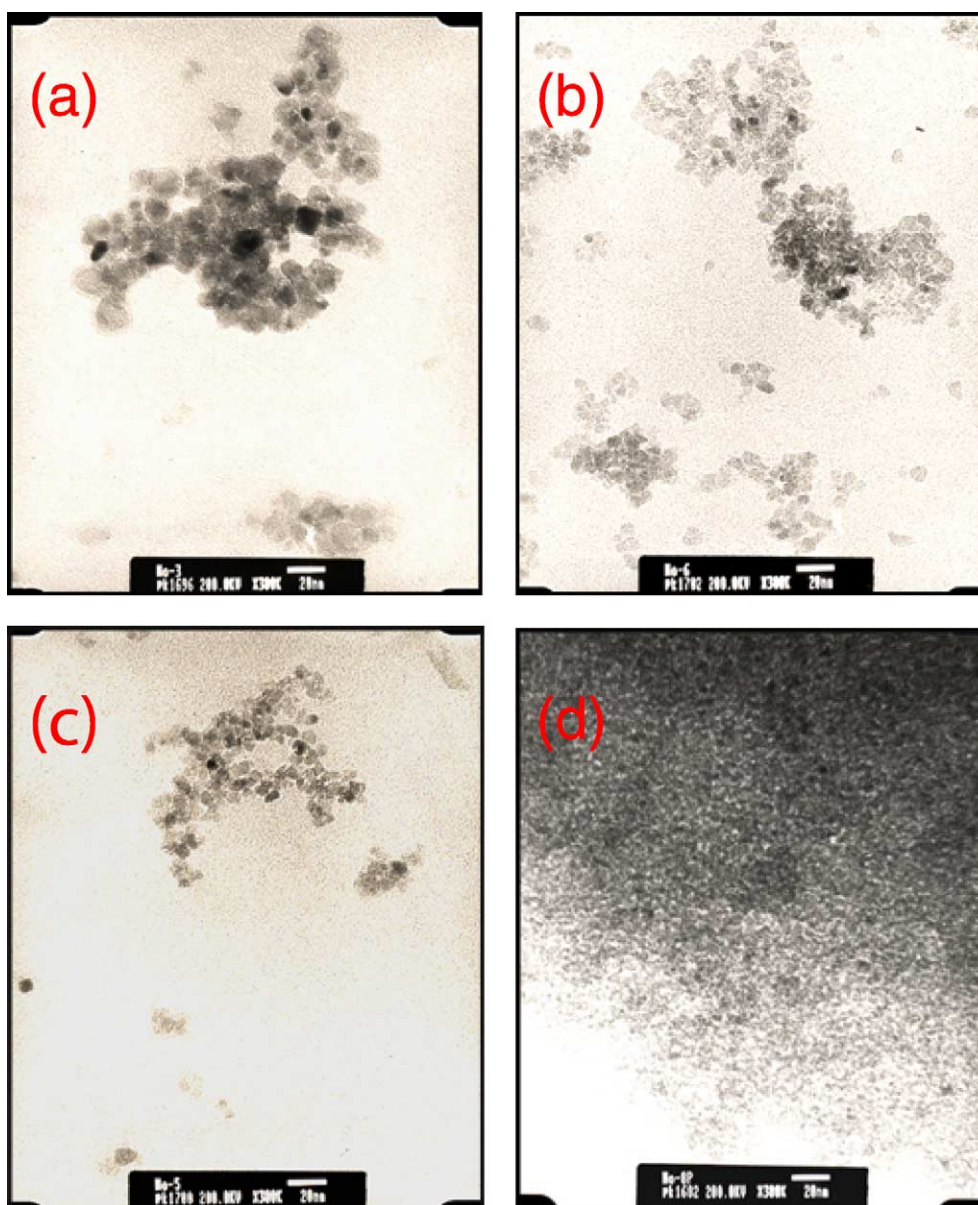


Fig. 4. TEM images of nanoparticles prepared at different TTIP/TEOS ratio: (a) $\text{TiO}_2 = 100$, (b) $\text{TiO}_2/\text{SiO}_2 = 90/10$, (c) $\text{TiO}_2/\text{SiO}_2 = 80/20$, and (d) $\text{TiO}_2/\text{SiO}_2 = 70/30$.

properties of the solute which depends on the reaction conditions, such as reaction temperature, pH of solution and the photocatalytic activity increases with increasing this value.

Table 2 shows the photocatalytic activity of *p*-nitrophenol on the pure TiO_2 and $\text{TiO}_2/\text{SiO}_2$ particles prepared by the microemulsion method.

The $\text{TiO}_2/\text{SiO}_2$ (90/10) particles shows the highest activity on the photocatalytic decomposition of *p*-nitrophenol. Up to 10% of SiO_2 amount, the photocatalytic activity increases with an increase of SiO_2 amount and has higher photocatalytic activity than that of pure TiO_2 particles but it decreases above 10% of SiO_2 content.

In addition, the pore volume of $\text{TiO}_2/\text{SiO}_2$ particles shows the highest values at the addition of 10 wt.% silica in titania (Table 2) and the pore size of $\text{TiO}_2/\text{SiO}_2$ (90/10) particles seems to be larger than those of $\text{TiO}_2/\text{SiO}_2$ (80/20 and 70/30) particles because the surface area increases continuously and pore volume decreases with an increase of silica content. Therefore, the large pore volume and pore size facilitate the mass transfer of reactants. From this result, it is thought that the increase of surface area by the formation of small pores is not always effective for high photocatalytic activity and the optimum composition of silica to titania was 10%.

4. Conclusion

Nanosized pure TiO_2 particles were prepared by hydrolysis of TTIP in the sodium bis(2-ethylhexyl) sulfosuccinate (AOT) reverse micelles. $\text{TiO}_2/\text{SiO}_2$ nanoparticles were also prepared from TEOS as a silicon source and TTIP as a titanium source. These particles were characterized and the photocatalytic decomposition of *p*-nitrophenol was also investigated using batch reactor in the presence of UV light. From thermal analysis and XRD analysis, the rutile structure of pure titania appeared above 700 °C but no rutile phase was observed for the $\text{TiO}_2/\text{SiO}_2$ particles up to 800 °C. It was also confirmed that the titania/silica mixture had high thermal stability, which results in the suppression of phase transformation of titania from anatase to rutile. The crystallite size of prepared particles decreased and the surface area monotonically increased with an increase of the silica content. From FT-IR analysis, the band for Ti–O–Si vibration was observed and the band intensity for Si–O–Si vibration increased with an increase of the silica content. The micrographs of TEM showed that

the $\text{TiO}_2/\text{SiO}_2$ nanoparticles had a spherical and a narrow size distribution. In addition, the crystallite sizes calculated from TEM analysis were nearly the same as those obtained from XRD analysis. $\text{TiO}_2/\text{SiO}_2$ particles showed higher photocatalytic activity than pure TiO_2 and the $\text{TiO}_2/\text{SiO}_2$ (90/10) particles showed the highest activity on the photocatalytic decomposition of *p*-nitrophenol.

Acknowledgements

This work was supported by Grant no. R01-2000-00323 from the Basic Research Program of the Korea Science & Engineering Foundation and Brain Busan 21 project.

References

- [1] R.W. Siegel, Ann. Rev. Mater. Sci. 21 (1991) 559.
- [2] K.C. Yi, J.H. Fendler, Langmuir 6 (1990) 1519.
- [3] H.C. Youn, S. Baral, J.H. Fendler, J. Phys. Chem. 92 (1988) 6320.
- [4] J.H. Fendler, Chem. Rev. 87 (1987) 877.
- [5] C. Petit, P. Lixon, M.P. Pileni, J. Phys. Chem. 94 (1990) 1598.
- [6] R. Leung, M.J. Hou, D.O. Shah, in: D.T. Wasan, M.E. Ginn, D.O. Shah (Eds.), Surfactant Science Series, vol. 28, Marcel Dekker, New York, 1988, p. 315.
- [7] V. Pillai, D.O. Shah, in: C. Soalns, H. Kunieda (Eds.), Industrial Application of Microemulsion, Marcel Dekker, New York, 1997, p. 227.
- [8] M.S. Lee, G.D. Lee, S.S. Park, S.S. Hong, J. Ind. Eng. Chem. 9 (2003) 89.
- [9] M.S. Lee, G.D. Lee, C.S. Ju, K.T. Lim, S.S. Hong, J. Korean Ind. Eng. Chem. 13 (3) (2002) 216.
- [10] C. Anderson, A.J. Bard, J. Phys. Chem. 99 (1995) 9882.
- [11] B.D. Cullity, Elements of X-ray Diffraction, Addison-Wesley, Reading, MA, 1978.
- [12] A. Duran, C. Serna, V. Fornes, J.M. Fernandez-Navarro, J. Non-Cryst. Solids 82 (1986) 69.
- [13] K.Y. Jung, S.B. Park, Appl. Catal. B 25 (2000) 249.